



Stern- und  
Planetenentstehung  
Sommersemester 2020  
Markus Röllig

Lecture 8: Stellar Clustering



[http://exp-astro.physik.uni-frankfurt.de/star\\_formation/index.php](http://exp-astro.physik.uni-frankfurt.de/star_formation/index.php)

## VORLESUNG/LECTURE

Raum: Physik - 02.201a

dienstags, 12:00 - 14:00 Uhr

## SPRECHSTUNDE:

Raum: GSC, 1/34, Tel.: 47433, (roellig@ph1.uni-koeln.de)

dienstags: 14:00-16:00 Uhr

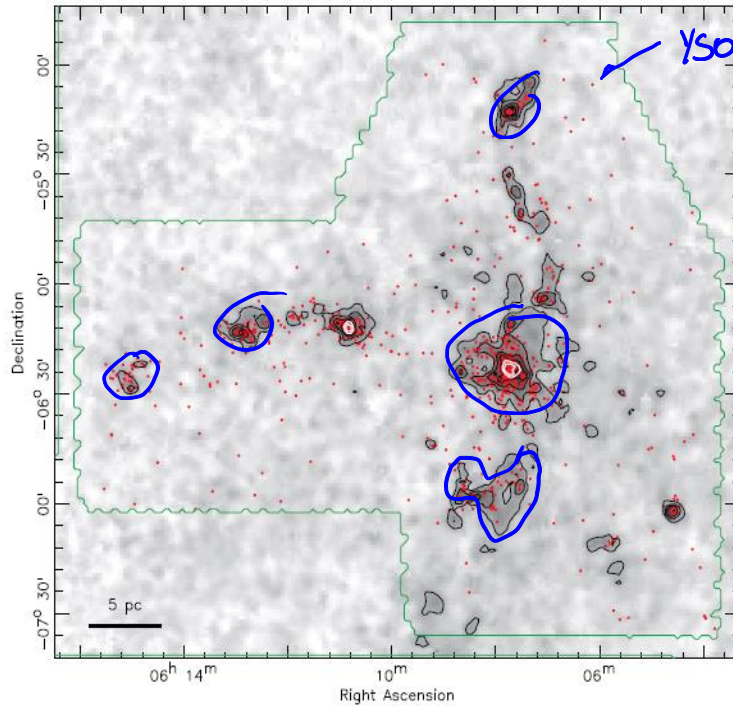
| Nr. | Thema   | Termin     |
|-----|---|------------|
| 1   | Observing the cold ISM  | 21.04.2020 |
| 2   | Observing Young Stars   | 28.04.2020 |
| 3   | Gas Flows and Turbulence<br>Magnetic Fields and Magnetized Turbulence | 05.05.2020 |
| 4   | Gravitational Instability and Collapse                                | 12.05.2020 |
| 5   | Stellar Feedback  | 19.05.2020 |
| 6   | Giant Molecular Clouds  | 26.05.2020 |
| 7   | Star Formation Rate at Galactic Scales                                | 02.06.2020 |
| 8   | Stellar Clustering  | 09.06.2020 |
| 9   | Initial Mass Function – Observations and Theory                       | 16.06.2020 |
| 10  | Massive Star Formation  | 23.06.2020 |
| 11  | Protostellar disks and outflows – observations and theory             | 30.06.2020 |
| 12  | Protostar Formation and Evolution                                     | 07.07.2020 |
| 13  | Late Stage stars and disks – planet formation                         | 14.07.2020 |

# 8 STELLAR CLUSTERING

How star formation is arranged (space & time) within a single MC.

## 8.1 OBSERVATIONS OF CLUSTERING

### 8.1.1 Spatial and Kinematic Distribution



young stellar objects

**Figure 1.** Extinction map of the MonR2 cloud overlaid in red with the spatial distribution of *Spitzer*-identified YSOs. The inverted gray scale is a linear stretch from  $A_V = -1$  to 10 mag. Contour overlays start at  $A_V = 3$  mag and their interval is 2 mag. The IRAC coverage is marked by the green boundary. The projected positions of the YSOs in MonR2 closely trace almost all of the areas of detectably elevated extinction. Denser clusters of YSOs are clearly apparent in the zones of highest extinction.

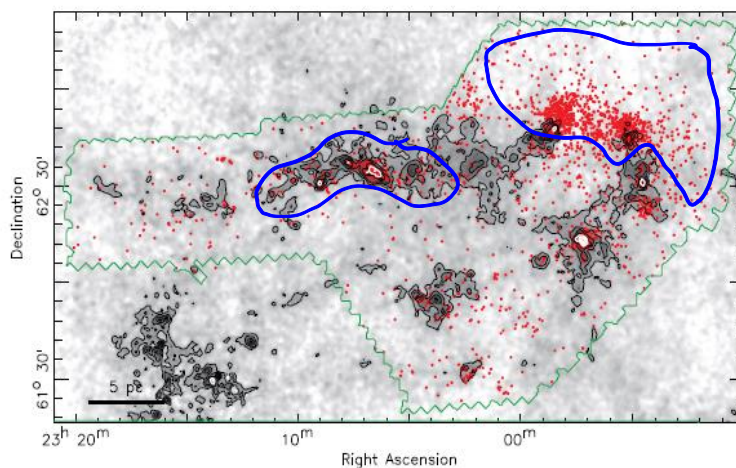


**Figure 2.** Extinction map of the CepOB3 cloud overlaid in red with the spatial distribution of *Spitzer*-identified YSOs. The gray-scale and contour properties are identical to those in Figure 1. As in that figure, YSOs are predominantly projected on the elevated extinction zones within the cloud, and clusters are found in the highest extinction zones. However, unlike MonR2, the large CepOB3b young cluster in the northwest corner of the coverage is largely offset from significant extinction. Focused examination of this region in particular suggests that the OB stars present have dispersed much of the local natal cloud material (Getman et al. 2009; T. S. Allen 2011, in preparation).



- use difference between true and random maps as measure of  $\xi(r)$
- alternatively measure mean surface density of neighbors as a function of distance:

$$\Sigma(r) = n[1 + \chi(r)]$$

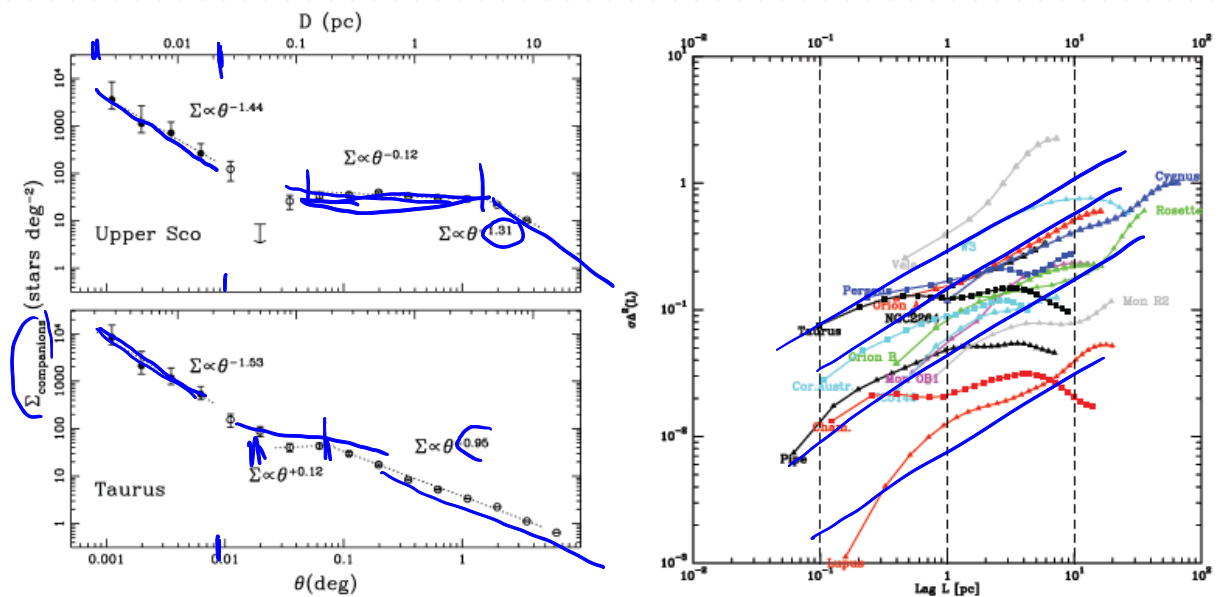


Abbildung 2 Measurements of the stellar and gas correlations in nearby star-forming regions. The two figures on the left show the surface density of neighbors around each star  $\Sigma(r)$  in Upper Sco and Taurus (Kraus & Hillenbrand, 2008). The right panel shows measurements, for a large number of nearby molecular clouds, of a statistic called the  $\Delta$  variance,  $\sigma_{\Delta^2}$ , which is related a measurement of structure on different scales that is related to the correlation function.

- stellar distribution
  - small separations -> power-law distribution
    - wide binaries
  - larger separations -> shallower falloff
    - distribution of stars in the cluster
    - power-law indicates self-similar, scale-free structures
    - index consistent with filamentary structure
- gas distribution
  - similar power-law structure
- gas and stars are in highly structured, fractal-like distributions
- young clusters: gas and stars strongly correlated
- older cluster: less correlation
- kinematics of gas and dust
  - stars and dense gas have lower velocity dispersions
  - less dense gas wider dispersion
  - mean velocity well correlated

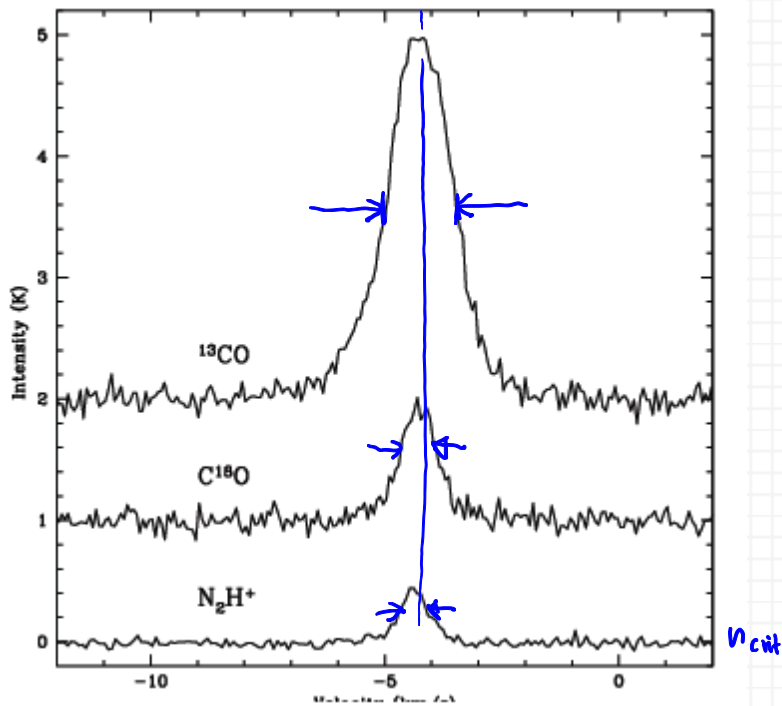


Abbildung 3 Velocity distribution toward a nearby protostellar core using three different molecular lines. The transitions  $^{13}\text{CO}$ ,  $\text{C}^{18}\text{O}$ , and  $\text{N}_2\text{H}^+$  should be roughly ordered from lowest to highest gas density.

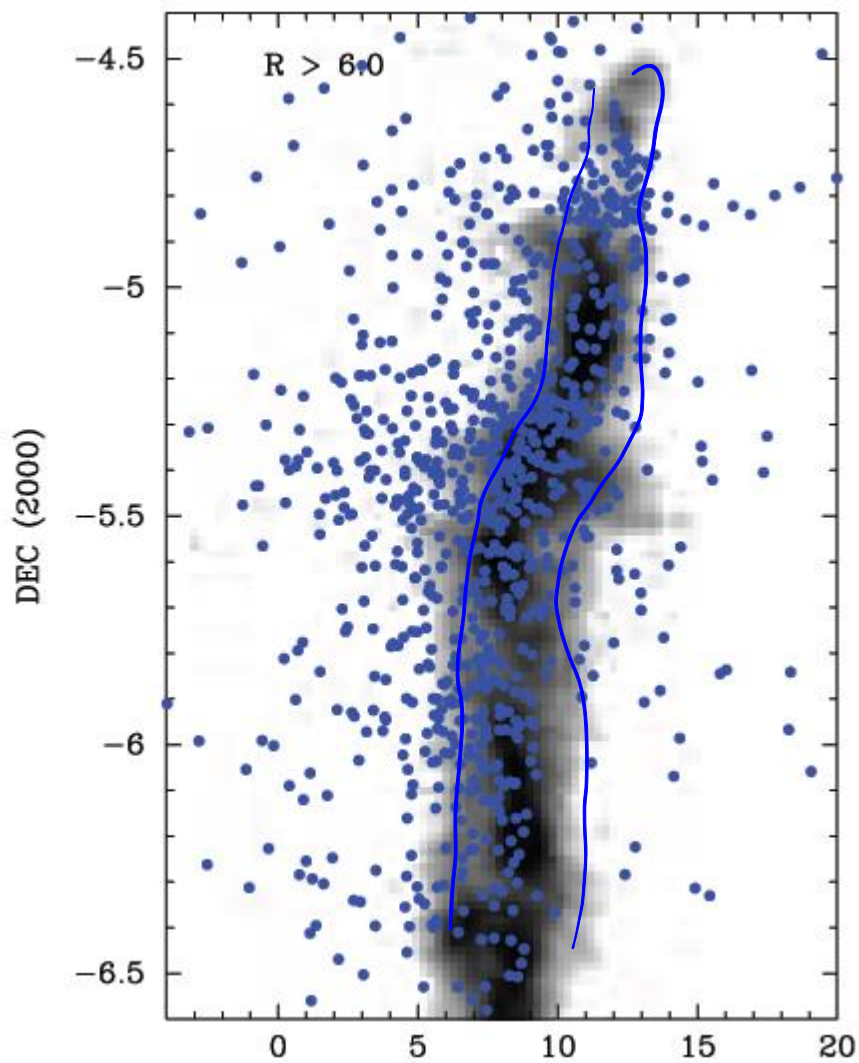


Abbildung 4 Measured distribution of  $^{13}\text{CO}$  (grayscale) and young stellar objects (blue points) in velocity (x-axis) and position on the sky in one dimension (y-axis) for the Orion Nebula Cluster

## 8.1.2 Time Evolution

- The younger the stellar population the better the star-gas correlation
- By stellar ages of  $\sim 5\text{-}10$  Myr, no associated gas at all
- typical SF environment much denser than average ISM
- newly formed star density much denser than average stellar density
  - $>90\%$  of SF activity within 2 kpc around sun takes place in regions where stellar mass density is larger than  $1M_{\odot}\text{pc}^{-3}$ , i.e.  $n > 30\text{ cm}^{-3}$  (Lada & Lada 2003)
  - stellar mass density in solar neighborhood  $\sim 0.01M_{\odot}\text{pc}^{-3}$  (Holmberg & Flynn 2000)
  - After 100 Myr, only 10% are in cluster with significantly higher densities, while 90% have dispersed!

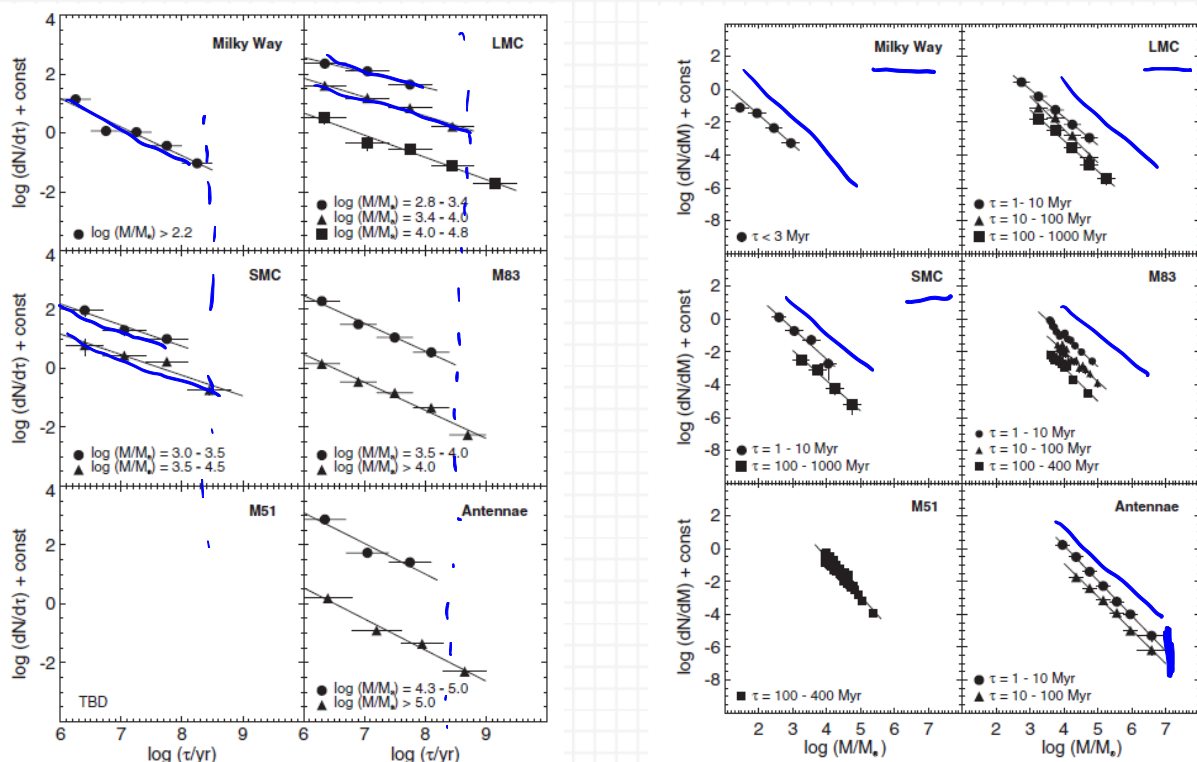


Abbildung 5 Fall & Chandar 2012

- Dispersion of stars indicates that formation was such that they were gravitationally unbound

- remaining star cluster show mass distribution according to

$$\frac{dN}{dM} \propto M^{-2}$$

## 8.2 THEORY

### 8.2.1 Origin of Gas and Stellar Distributions

- Spatial and kinematic distribution a result of cold gas behavior
  - gravitational collapse at free-fall time  $t_{ff} \propto \rho^{-1/2}$
  - runaway collapse in densest regions where stars form first
  - highly concentrated structure with stars at the densest spots
- Simulations of turbulent flows are able to reproduce the observed two-point correlation functions
- Kinematics explained by turbulent condensation
  - strong converging shocks produce densest regions
  - after such a shock velocities are small because opposing velocities cancel
  - densest gas has low velocity dispersion
  - stars inherit the gas kinematics





- Simulations reproduce the kinematics

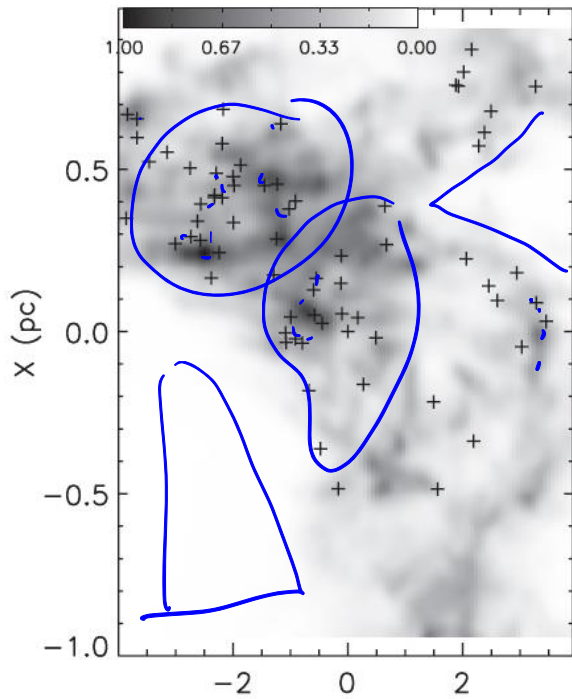


Abbildung 6 Distributions of  $^{13}\text{CO}$  and YSO in velocity and position in a simulation of the Orion Nebula Cluster (Offner et al. 2009)

## 8.2.2 Gas Removal and Transition to Gas-Free Evolution

- Low mass SF can be well described by gravity + hydrodynamics
- transition to gas-free evolution not well described (because stellar feedback now crucial)
- Without feedback:
  - SF rates of factor 100 too high
  - all gas transformed into stars ●
  - if parental cloud was bound then stellar cluster is also bound
  - even if cloud is unbound
  - bound sub-regions will form bound cluster that remain bound internally even if unbound from other sub-cluster
- observation that most stars end up unbound requires to truncate SF before all gas is used up

### 8.2.2.1 Rapid versus Adiabatic Mass Loss

What happens to a system in equilibrium if mass is removed? Consider a system (stars and gas) with mass  $M$  in virial equilibrium

$$2\mathcal{T} + \mathcal{W} = 0$$

Reduce mass from  $M$  to  $\epsilon M$  (due to some stellar feedback) rapidly (no adjustment of the system)  $\epsilon$ : fraction of mass turned into stars

Then new kinetic energy is  $\mathcal{T}' = \epsilon \mathcal{T}$

New potential energy is  $\mathcal{W}' = \epsilon^2 \mathcal{W}$

New total energy:

$$E' = \mathcal{T}' + \mathcal{W}' = \epsilon \mathcal{T} + \epsilon^2 \mathcal{W} = \epsilon(1 - 2\epsilon)\mathcal{T} = \epsilon \left( \epsilon - \frac{1}{2} \right) \mathcal{W}$$

$\mathcal{T} > 0$  and  $\mathcal{W} < 0$  therefore, the new energy is only negative (i.e. system is still bound) if  $\epsilon > 1/2$ .

If the system remains bound, it will establish a new radius:

$$R' = \frac{\epsilon}{2\epsilon - 1} R$$

Adiabatic Mass Loss: Re-establish equilibrium after each incremental mass loss  $dM$

$$R' = \frac{\epsilon}{2\epsilon - 1} R = \frac{1 + dM/M}{1 + 2dM/M} R = \left[ 1 + \frac{dM}{M} + \mathcal{O}\left(\frac{dM^2}{M^2}\right) \right] R$$

$$\frac{dR}{R} = \frac{R' - R}{R} = -\frac{dM}{M}$$

$$\ln R = -\ln M + \text{const}$$

$$R' \propto \frac{1}{M}$$

- rapid gas removal &  $\epsilon < 50\%$ : unbound cluster
- slow gas removal &  $\epsilon > 50\%$ : bound cluster

Very simplifying. Ignoring:

- energy is not distributed perfectly among stars
- cluster embedded in galactic grav. potential that pulls of outskirts
- stars have distribution of dense gas -> more difficult to unbind

### 8.2.3 Cluster Formation Efficiency

Consider spherical gas cloud with mass  $M$  and radius  $R$  that begins forming stars.

SF ends, when stars inject enough momentum into cloud to accelerate gas up to escape velocities

$$v_e \sim \sqrt{\frac{GM}{R}}$$

Stellar mass at any given time is  $\epsilon M$ , then momentum injection rate is

$$\dot{p} = \left\langle \frac{\dot{p}}{M_*} \right\rangle \epsilon M$$

SF ceases when

$$M v_e \sim \dot{p} t_{cr} \sim \left\langle \frac{\dot{p}}{M_*} \right\rangle \epsilon M \frac{R}{v_e} \quad t_{cr} \sim R/v_e$$

$$\epsilon \sim \left\langle \frac{\dot{p}}{M_*} \right\rangle^{-1} \frac{v_e^2}{R} \sim \left\langle \frac{\dot{p}}{M_*} \right\rangle^{-1} \frac{1}{2} G \Sigma \quad \Sigma \sim M/R^2$$

For  $\epsilon = 1/2$  this gives

$$\left\langle \frac{\dot{p}}{M_*} \right\rangle \sim G \Sigma$$

For radiation feedback:  $\left\langle \frac{\dot{p}}{M_*} \right\rangle = 23 \text{ km s}^{-1} \text{ Myr}^{-1}$

This gives  $\Sigma \sim 1 \text{ g cm}^{-2}$

Regions with surface densities of  $1 \text{ g cm}^{-2}$  or higher should be able to form bound clusters. (Much higher than most regions!) See Kruijssen 2012.

## 8.2.4 Cluster Mass function

What are the implications of this sort of analysis for the cluster mass function?

Consider a collection of star-forming gas clouds with an observed mass spectrum  $\frac{dN_{obs}}{dM_g}$ . Each such cloud lives for a time  $t_l(M_g)$  before forming its stars and dispersing, so the cluster formation rate is

$$\frac{dN_{form}}{dM_g} \propto \frac{1}{t_l(M_g)} \left( \frac{dN_{obs}}{dM_g} \right)$$

Now let  $\epsilon$  be the final star formation efficiency for a cloud of mass  $M_g$ , and let  $f_{cl}(\epsilon)$  be the fraction of the stars that remain bound following gas removal.  $\rightarrow$  final mass of star cluster formed will be

$$M_c = f_{cl} \epsilon M_g$$

$\rightarrow$  formation rate for star clusters of mass  $M_c$

$$\begin{aligned} \frac{dN_{form}}{dM_c} &= \left( \frac{dM_c}{dM_g} \right)^{-1} \left( \frac{dN_{form}}{dM_g} \right) \\ &\propto \left[ \epsilon f_{cl} + \left( f_{cl} + \frac{df_{cl}}{d \ln \epsilon} \right) \left( \frac{d \epsilon}{d \ln M_g} \right) \right]^{-1} \left( \frac{1}{t_l(M_g)} \right) \left( \frac{dN_{obs}}{dM_g} \right) \propto M^{-2} \end{aligned}$$

Translation of observed cloud mass into formation rate of cluster of several masses.

$\left( \frac{1}{t_l(M_g)} \right)$ : accounts for the fact that our observed catalog of clouds oversamples the clouds that stick around the longest

$\epsilon f_{cl}$ : translates from gas cloud mass to cluster mass

$\left(f_{cl} + \frac{df_{cl}}{d \ln \epsilon}\right) \left(\frac{d\epsilon}{d \ln M_g}\right)$ : compensates for the way the gas cloud mass

function gets compressed or expanded due to any non-linear mapping between gas cloud mass and final star cluster mass.

Observations:  $\frac{dN}{dM} \propto M^{-2}$  therefore the term in [...] cannot be a strong function of  $M_g$ .

Thus, star formation efficiency  $\epsilon$  cannot be a very strong function of gas cloud mass!